A novel comb-like copolymer based polymer electrolyte for Li batteries

Mingkui Wang, Li Qi, Feng Zhao, Shaojun Dong*

State Key Laboratory of Electroanalytical Chemistry, Changchun Institute of Applied Chemistry, Chinese Academy of Sciences, Changchun 130022, China

Abstract

Polymer electrolytes, which comprise a novel comb-like copolymer and an alkali metal salt, were successfully prepared and discussed using differential scanning calorimeter, Fourier transform infrared spectroscopy, nuclear magnetic resonance, atom force microscopy, and electrochemical impedance spectroscopy. The novel comb-like copolymer is capable of forming donor:acceptor type bonds with alkali metal ions. The complex system with a mixture of fumed silica or propylene carbonate was studied also. Such electrolytes possess satisfactory ambient temperature ionic conductivity (up to 10^{-4} S cm^{-1}) and good mechanical strength. The Vogel–Tamman–Fulcher-like behavior of conductivity implies the coupling of the charge carriers with the segmental motion of the polymer chains.
© 2004 Elsevier B.V. All rights reserved.

Keywords: Ionic conductivity; Polymer electrolyte; Impedance spectroscopy

1. Introduction

There is presently a great demand for solid polymer electrolytes that combine high ionic conductivity, electrochemical stability, and good mechanical properties for use in high-energy density batteries and other applications [1]. Basically, the conducting polymeric matrices contain two key elements: polymers possessing appropriate functional groups that can interact with ions, and electrolytes which, in many cases, are the same as those used in liquid solutions. PEO-based electrolytes are the earliest and the most extensively studied systems [2]. The ether oxygen acts as coordinating site in the system that promotes the dissociation of the salt [3–5]. Although such complexes show high ionic conductivity at high temperature, the properties for crystallization of polymers at low temperatures severely reduce their conductivity. Recently, gel polymer electrolytes with high ionic conductivity of about 10^{-3} S cm^{-1} at ambient temperature have been re-

ported. The typical examples of such electrolytes were those on poly(methyl methacrylate), poly(vinylidene difluoride), and poly(acrylonitrile) [6–9]. These systems are composed of functional groups that are not sufficient to create charge separation between electrolyte ions. Thus, special additives are required to promote sufficient charge separation, which enable the ions in the solid matrix to respond to an electric field. In these systems, the major role of the polymer is mostly to maintain a solid and stable matrix, whereas the ion migration within the matrix under an electrical field is feasible because of the additives. However, the mechanical property of such polymer electrolytes is generally very poor because of the characteristic of gels and additives.

Several approaches to overcome the problems mentioned above have been outlined in some literatures [10–13]. For example, crystallization can be largely avoided by the use of polymer architectures where short PEO chains are attached as pendant chains to backbone polymers [14]. The mechanical stability can be improved by forming rigid cross-linked networks, for example, by UV irradiation of reactive multifunctional PEO oligomers [15,16]. By these attractive ways, solid

* Corresponding author. Tel.: +86 431 5261011; fax: +86 431 5689711.
E-mail address: dongsj@ciac.jl.cn (S. Dong).

polymer electrolyte materials with high mechanical strength have been obtained. These materials belong to the class of "hairy rod molecules" [17], which have a strong tendency to self-organize into supramolecular architectures when cast from solution. The use of such materials as separators in Li batteries offers the advantage of minimizing the separator thickness and thus the internal electrical resistance of cells. But some disadvantages of such material may be its electrochemically instability, such as hydroxyl end-groups of PEO oligomers reacting with lithium metal [18], and so on.

In the current study, polymer electrolytes based on a novel comb-like copolymer were prepared and investigated. The comb-like copolymer was prepared by copolymerization of poly(ethylene glycol) methyl ether methacrylate (PEG-MEMA) with acrylonitrile (AN) and methyl methacrylate (MMA) according to their several advantages [19–22]. It was anticipated that these modified polymers would form continuous networks by interpolymer aggregation through microphase separation of the chain end segments, and have high ionic conductivity with good mechanical strength. Such solid polymer electrolytes including lithium perchlorate were prepared and characterized. The complex system with a mixture of SiO_2 or propylene carbonate (PC) was studied also. The chemical and electrochemical properties of the composite polymer electrolytes were studied using differential scanning calorimeter (DSC), Fourier transform infrared (FT-IR), nuclear magnetic resonance (NMR), atom force microscopy (AFM), and electrochemical impedance spectroscopy (EIS).

2. Experimental

2.1. Materials and pretreatment

The starting compounds, poly(ethylene glycol) methyl ether (PEGME, average M_n ca. 350), methacrylic acid (MA), acrylonitrile (AN), methyl methacrylate (MMA), and $LiClO_4$ (99%) were purchased from Aldrich Chemical Company. The hydrophobic fumed silica (SiO_2 12 nm primary particle size) was purchased from Fluka Chemika. *N,N*-dimethylformamide (DMF, analytical reagent) was obtained from Beijing Chemical Reagent Company, China. PEGME, AN, and DMF were dried by using molecular sieves type 4 Å under reduced pressure at 30 °C for about 72 h. MMA was distilled under reduced pressure. $LiClO_4$ was dried at 120 °C and SiO_2 at 80 °C under vacuum for 48 h prior to use, respectively.

2.2. Synthesis of comb-like copolymer

The synthesis of PEGMEMA and PEGMEMA–AN–MMA copolymer was schematically shown in Scheme 1. Compound (a) PEGMEMA was obtained as described previously [21,22]. At first, PEGME was added to a benzene solution of MA that was mixed at about 80 °C in a glass flask, then, an inhibitor, 1,3-benzenediol, was homogenized
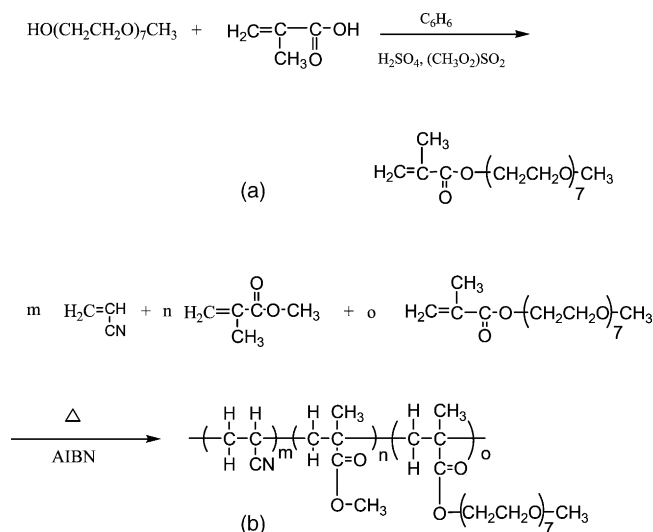
Scheme 1. Synthesis of comb-shaped copolymer.

with PEGME while keeping heating. After the inhibitor dissolved completely, a mixture with special ratio including MA (MA:PEGME=2:1, mole ratio), benzene (solvent), concentrated sulfuric acid and dimethyl sulfate (catalyzer) were added into the flask in turn. The reaction was carried out under the control of temperature. After the esterification reaction finished completely, the crude product was washed with alkaline liquor till to pH 7, and then with redistill water till to colorless. When the solution was removed under reduced pressure at about 50 °C, the end product, PEGMEMA was obtained.

Compound (b), PEGMEMA–AN–MMA copolymer was obtained by polymerization of PEGMEMA, AN, and MMA with special ratio under nitrogen atmosphere, in which AIBN was used as the catalyzer. The polymerization was continued at 30–45 °C for 24 h, and then kept at 60 °C for another 24 h. The end product, PEGMEMA–AN–MMA copolymer was obtained.

2.3. Sample preparation and measurements

The prepared copolymer materials were dissolved in DMF to make copolymer + $LiClO_4$ complexes. The content of $LiClO_4$ ranges from 0.1 to 2 mol kg^{-1} of copolymer. The hybrid electrolytes were obtained by dispersion of SiO_2 in a copolymer + $LiClO_4$ solution. The concentration of SiO_2 in the hybrid electrolytes was equal to 10 wt.%. All percentages for the plasticizer, quoted in this paper, were normalized with respect to the weight of the copolymer. The hybrid membrane was cast on a glass plate, and slowly dried by an infrared light until a uniform and freestanding membrane with good mechanical strength was gotten. The casting membranes were then kept under vacuum (6.67 Pa) for 24 h at 70 °C before use. The preparation of samples was performed in a dry-box (M. Braun, GmbH, Germany) filled with nitrogen, in which moisture condition was lower than 1 ppm.

Thermal behavior of the hybrid and complex membranes were studied by means of DSC using PERKIN-ELMER 7 Series Thermal Analysis System. The samples were loaded in sealed aluminum pans, and measurements were heated from -60 to $160\,^{\circ}\text{C}$ at $10\,^{\circ}\text{C}\,\text{min}^{-1}$ under nitrogen atmosphere.

Sample was prepared on a KBr pallet for FT-IR study by solvent casting. Infrared spectra were obtained with a FT-IR spectrophoto meter (Nicolet FT-IR-520FT) and recorded by averaging 64 scans with a wavenumber resolution of $2\,\text{cm}^{-1}$.

High-resolution ^{1}H NMR measurements were performed on a Bruker 600 spectrometer. The comb-like copolymer was dissolved in dimethyl sulfoxide. The ^{1}H chemical shifts were referenced relative to tetramethylsiliane at 0.0 ppm.

AFM imaging was carried out in a contact mode (Digital Instruments Nanoscope III), using a 14 μm scanner along with Si cantilevers and a silicon nitride tip (Digital Instruments model NP). Each image was composed of 256 pixels in each direction in the plane of the surface.

Conductivity measurements were carried out using Autolab with PSGTAT 30 (Eco Chemie, The Netherlands) with the help of frequency response analysis (FRA) system software under an oscillation potential of 10 mV over a frequency range of 1 MHz to 0.1 Hz. A laboratory-built Teflon cell holder with stainless steel electrodes (SS 304) was used. An ac impedance experiments were performed on the cells in the temperature range of 25–80 °C. All samples within the holder were subjected to heat treatment at 60 °C for 24 h and then cooled slowly to room temperature. The cell holder was then introduced into a dry-bath thermostat especially designed for these experiments, which calibration gave the samples temperature within $\pm0.25\,^{\circ}\text{C}$. The cell was left for 1 h to reach thermal equilibrium before each experiment. The thickness of membranes was about 50–100 μm, and the area was about $1.77\,\text{cm}^2$.

3. Results and discussion

Well-characterized comb-like copolymers were prepared by the two-step procedure as shown in Scheme 1. The first step involved the preparation of a PEGMEMA branched chain by reaction of PEGME and MA [21,22]. The second step was the polymerization of PEGMEMA, AN, and MMA. The synthesis process was followed with FT-IR spectroscopy (Fig. 1). The assignment of the main absorption bands appearing in the FT-IR spectrum is listed in Tables 1 and 2. Characteristics in the spectrum of PEG-
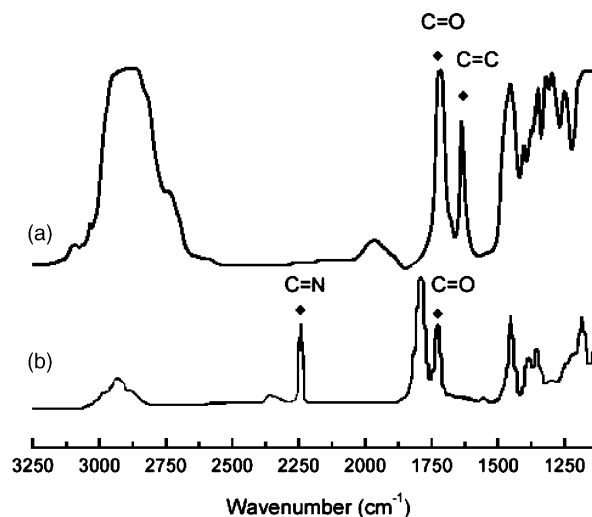

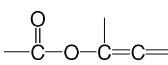Fig. 1. IR spectra for (a) PEGMEMA, and (b) copolymer (PEGMEMA–AN–MMA, n:m:o=1:18:1).

MEMA are C=O bands at 1718 cm^{-1} together with C–O–C bands at 1108 cm^{-1}, as shown in Fig. 1a. The FT-IR spectrum in Fig. 1b shows the characteristic absorption peaks of C≡N groups at about 2242 cm^{-1}, while the C=C bands at 1637 cm^{-1} found to be absent, indicating that the polymerization of AN and MMA to PEGMEMA has been processed. ^{1}H NMR spectrum of the synthesized comb-like copolymer is shown in Fig. 2. The peaks at 2.028–2.144 ppm were assigned to methylene (CH$_2$) protons in the MMA, AN, and PEGMEMA units. The methoxy protons linked to the adjacent carbonyl group in the MMA unit was found at 3.649–3.671 ppm. The peaks appearing at 1.329 ppm correspond to methyl (CH$_3$) protons in the MMA and PEGMEMA units. The peak of DMSO-d appeared at 2.507 ppm. Both FT-IR and NMR spectra reveal that a comb-like copolymer with a special design on the side chain has been successfully synthesized.

In view of the permittivity and the softness of the polymer chain and mechanical properties of the copolymer, PEGMEMA–AN–MMA copolymer (m:n:o = 18:1:1, $P = 7$) is used to as the matrix of polymer electrolyte for lithium batteries [21–23]. The material exhibits good film formation, solution maintaining capacity, and dimensional stability. The composition of various polymer electrolytes based on the copolymer was listed in Table 3. In this study, four polymer electrolytes were cast to thin membranes with following composition:

Table 1
Assignment of the main vibrational bands in the FT-IR spectrum of PEGMEMA

Wavenumbers (cm^{-1})	Strength	Vibration
∼2872	Strong, wide (asymmetry)	C–H in CH$_3$ and CH$_2$
∼1718	Very strong, wide	C=O in α, β unsaturated acid esters
1637	Strong, sharp	C=C in polymer backbone
1453	Middle, sharp	C–H in the overlap of CH$_3$ and CH$_2$
∼1170	Strong, wide (asymmetry)	C–O in α, β unsaturated acid esters

Table 2
Assignment of the main vibrational bands in the FT-IR spectrum of PEGMEMA–AN–MMA

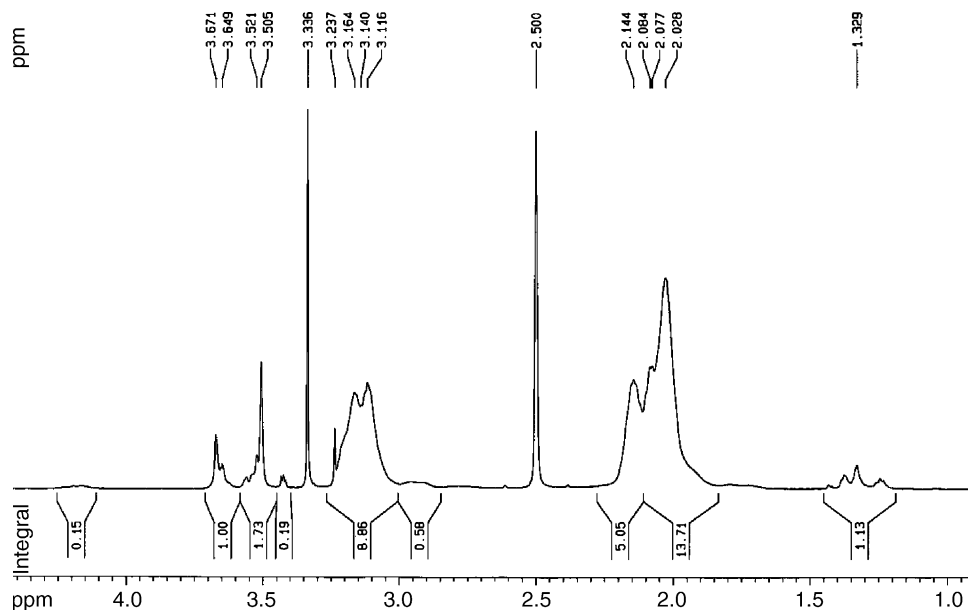| Wavenumbers (cm^{-1})	Strength	Vibration
~2883	Strong, wide (asymmetry)	C≡H in CH_3 and CH_2
2242	Strong, sharp	C≡N
1796–1789	Strong, wide	C=O in $-\overset{\displaystyle O}{\overset{\displaystyle \|}{C}}-O-\overset{\|}{C}=C=$
1732–1722	Very strong, wide	C=O in α, β unsaturated acid esters
1167	Strong, weak (asymmetry)	C−O in α, β unsaturated acid esters

Fig. 2. ^{1}H NMR spectra of comb-like copolymer (sample b in Fig. 1).

S1: copolymer + LiClO$_4$;
S2: copolymer + LiClO$_4$ + PC (PC: 50%);
S3: copolymer + LiClO$_4$ + SiO$_2$;
S4: copolymer + LiClO$_4$ + SiO$_2$ + PC (PC: 50%);

Fig. 3 presents DSC curves for the copolymer–LiClO$_4$–SiO$_2$ system. There is no crystallization endotherm in the temperature range. For the copolymer sample, the glass transition temperature (T_g) occurs at 50.8 °C. The sample S1 has higher T_g (76.7 °C) than that of the sample S3 (73.8 °C). The results indicate interactions existed between the copolymer body and additives. The interactions cause the ascending T_g of hybrid polymer and have an important effect on ionic conductivity [23].

Fig. 4 shows AFM micrographs of polymer membranes using (a) copolymer and (b) copolymer + SiO$_2$. All AFM images exhibit smooth surface, whose characteristic features depend on the composite of membranes. The membrane has obviously porous structure and rough surface when SiO$_2$ was added. This phenomenon implies that the membrane without SiO$_2$ shows higher density. It results mainly from the difference in the speed of solvent evaporation during the formation of the polymer membranes. The nanosized hydrophobic fumed silica, due to its large surface area and special surface function, can readily absorb particles around it and then improve the membranes mechanical strength. It may be also emphasized that during DMF evaporation, the increased viscosity of the polymer matrix fixed the distribution of SiO$_2$
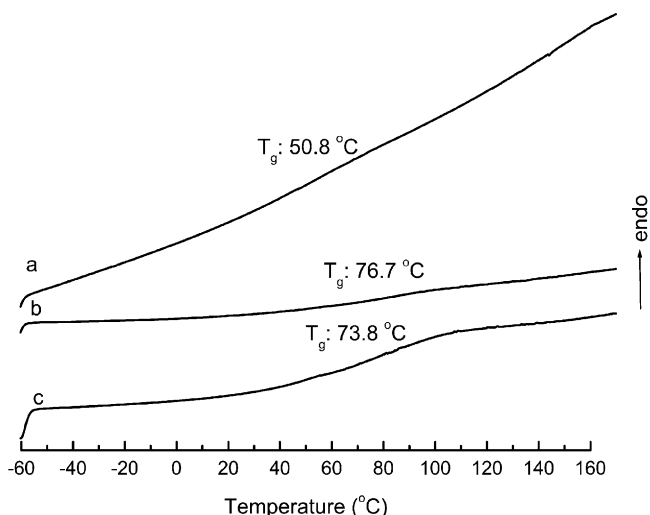
Table 3
Ionic conductivities of the composite copolymer electrolyte at 25 °C

Li$^+$ content sample (mol kg^{-1})	Ionic conductivity (S cm^{-1})				
	0.1	0.5	1.0	1.5	2.0
S1	a	a	1.31×10^{-9}	2.27×10^{-9}	1.51×10^{-8}
S2	1.21×10^{-9}	9.44×10^{-6}	7.33×10^{-6}	1.47×10^{-5}	1.32×10^{-5}
S3	2.27×10^{-11}	2.18×10^{-9}	8.40×10^{-9}	4.03×10^{-9}	3.75×10^{-8}
S4	8.71×10^{-8}	1.89×10^{-5}	3.64×10^{-5}	4.16×10^{-4}	1.89×10^{-4}

[a] It is difficulty to calculate ionic conductivity with the ac impedance spectrum.

Fig. 3. DSC curves of the composite polymer films: (a) copolymer; (b) copolymer + LiClO$_4$; (c) copolymer + LiClO$_4$ + SiO$_2$.

particles. In this way, substantial solvent DMF was absorbed on the surface of SiO$_2$. Those absorbed solvent evaporate slowly and then create pores as shown in Fig. 4b. The polymer backbone chain is composed of MMA and AN, which can swell in PC [9]. These polymer films become swelling and gel and show more softly surface after impregnated with PC. The soft films cannot show clear AFM image when the contact model was used in AFM measurement.

In order to understand the conductive behavior of the polymer electrolyte, EIS analysis of different membranes was performed. The typical impedance plots (Nyquist form) for the composite polymer electrolyte are shown in Fig. 5. There are two kinds of curves in these plots with the frequency range of 1 MHz to 0.1 Hz. As illustrated in the inset of Fig. 5a, the profile shows a depressed semicircle starting from the origin of the plot in the high frequency range and a straight line inclined at constant angle to the real axis in the low frequency range. When the hybrid polymer electrolyte impregnated with PC,
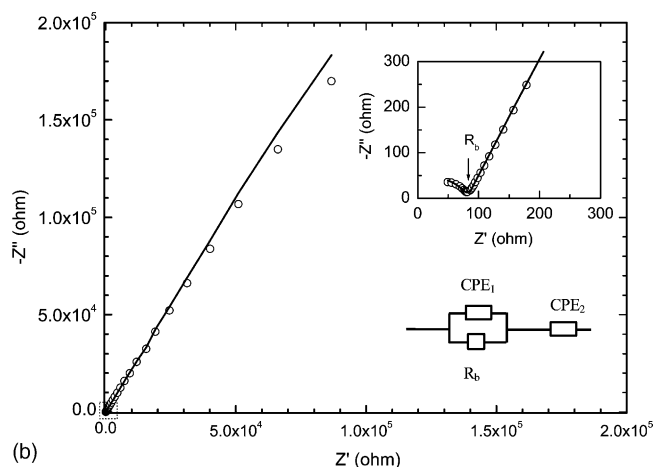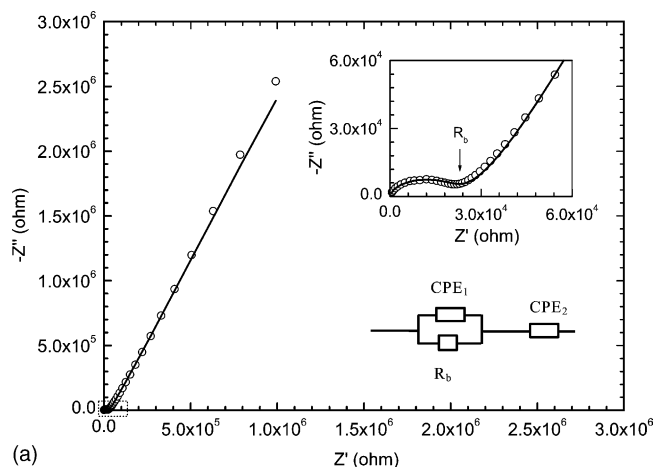

Fig. 5. Alternating current impedance spectrum of SS/polymer electrolyte/SS cell at 25 °C in Nyquist form for the composite film (a) without PC and (b) with PC. Simulated curves are shown as solid lines. Its corresponding equivalent circuit and the enlarged data in high frequency are shown in inset. Symbols Z' and Z'' refer to real component and imaginary component. R_b stands for the resistances of Li ion migration in electrolyte bulk; CPE$_1$ and CPE$_2$ are associated with the bulk-electrolyte and the double-layer capacitances, respectively.
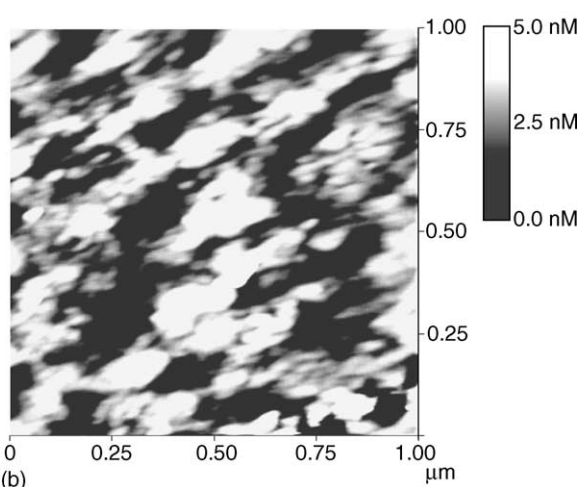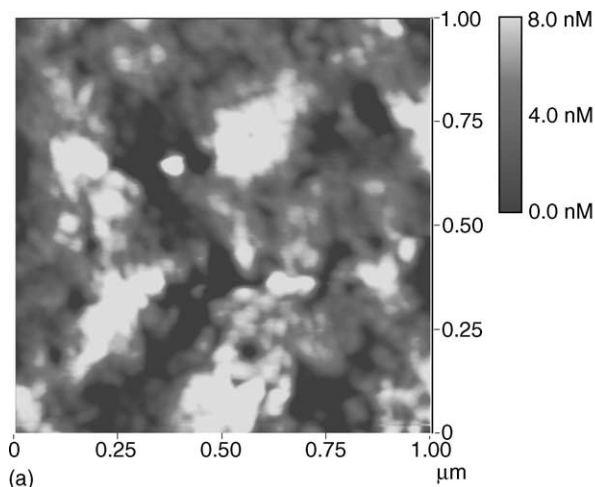

Fig. 4. AFM images of different membranes (a) copolymer membrane, and (b) copolymer membrane with SiO$_2$.

the impedance spectra shown in Fig. 5b depicts an approximately straight line starting from the real axis in the high frequency region. In fact, an incomplete semicircle could be seen in the inset of Fig. 5b, which also suggests the capacitive behavior at the higher frequency range. As for the blocking electrode used in the experiment [24], conductive ions cannot easily cross through the interface of electrode/electrolyte. The conductive ions accumulate near the interface when an electric field was applied. Ion concentration gradient will grow up in this situation, which impedes the further diffusion of conductive ions until an equilibrium state reaching. A single equivalent circuit as shown in the inset of Fig. 5 was used to describe the results. The equivalent circuit consists of a parallel circuit of CPE_1 and the bulk electrolyte resistance (R_b) in series with CPE_2. The CPE_1 and CPE_2 may be associated with the bulk electrolyte and the double layer capacitances, respectively.

The constant phase element (CPE) was necessarily introduced to account for the non-ideality of the interface between the electrode and electrolyte in the practical impedance spectrum, especially for the rough geometry interface [25,26]. The impedance of a CPE can be expressed as following:

$$Z_{CPE} = A(j\omega)^{-n} \tag{1}$$

$$\alpha = (1 - n)\frac{\pi}{2} \tag{2}$$

where $A = C^{-1}$ only when $n = 1$, and n is related to α (the deviation from the vertical of the line in the Z'–Z'' plot), $n = 1$ indicates a perfect capacitance, and lower n values directly reflect the roughness of the electrode used.

Hence, with the help of the FRA system software, the equivalent circuit was used to fit the experiment data. The bulk electrolyte resistance R_b and CPE can be estimated from this fitting procedure. The ionic conductivity σ of the polymer electrolyte is calculated by

$$\sigma = \frac{l}{AR_b} \tag{3}$$

where l is the thickness of the blend polymer electrolyte film and A is the area of the SS electrode.

The ionic conductivity of different membranes was list in Table 3. The largest ionic conductivity of S1 is Li^+ ion content increasing to 2.0 mol kg^{-1}. After the addition of SiO_2, ionic conductivity of hybrid membranes S3 increases slightly than that of S1. The gel membranes S4 prepared with SiO_2 show the highest conductivity, which have a conductivity up to 10^{-4} S cm^{-1} at 25 °C. The increasing of ionic conductivity could be attributed to the addition of SiO_2, especially for the gel polymer electrolytes. These facts consist with the explanation in details described by Petrucci and Eyring [27]. For the composite polymer electrolyte containing SiO_2 filler and/or PC plasticizer, the larger of ionic conductivity indicts the increasing of charger carriers and the decreasing of viscosity in the composite system.

Table 4
Lithium ionic content dependence of C_g obtained from CPE_1 for the composite polymer electrolyte at 25 °C

Li^+ content sample (mol kg^{-1})	C_g (pF)				
	0.1	0.5	1.0	1.5	2.0
S1	96	120	102	116	107
S2	130	439	1960	1740	626
S3	39	51	36	58	60
S4	409	582	409	639	599

In the same way, the geometric capacity (C_g) of the bulk polymer electrolyte obtained from CPE_1 are list in Table 4, which is related to cationic migration and dielectric polarization according to the corresponding Nyquist figure. As shown in Table 4, the capacity C_g increased after the hybrid polymer electrolyte impregnated with PC, but decreased after the addition of SiO_2.

In order to relate the equivalent circuit to the copolymer + salt composite systems, it is reasonable to speculate on a schematic structure for lithium salt in the copolymer systems. According to our design, the copolymer has stiff chains (AN and MMA) as reinforcing backbone moieties for good mechanical strength and flexible side chains (PEGMEMA) as the liquid matrix for ion transport. In the novel comb-like copolymer system, lithium perchlorate can be easily dissociated into cations and anions, which are dispersed and stabilized by oxygen atoms and methylene groups in the copolymer chains, respectively. The lone pair electron of oxygen can form donor:acceptor type bonds with Li^+ ions, which lowers the cationic transport number, and induces the increase of T_g of the composite membranes as illustrated in Fig. 3. When an additional potential is applied, cations tend to move towards the cathode while anions move in the opposite direction. At the same time, the charges on the interface of electrode and electrolyte will rearrange. It is well known to all, the capacity of C_g is related to the diffusion of these ions mobility, which can be analyzed from EIS as mentioned above. When SiO_2 was added, the interaction between lone pair of oxygen and Li^+ ion was influenced by nano-SiO_2 for the particle effect. The ionic conductivity increases slightly as shown in Table 3, but the capacity decreases as shown in Table 4 for the change of permittivity. When the hybrid polymer film was swelled with the high permittivity PC, the conductivity increases highly. The decreasing charge density on the surface of Li^+ ions reduces the interaction between lone pair and Li^+ ion when PC added. Especially, the polymer electrolytes with SiO_2 have more obvious effect when impregnated with PC.

To characterize the transport properties of the electrolyte more fully, the study of ionic conductivity as a function of temperature is also used. Fig. 6 depicts temperature dependence of the ionic conductivity of polymer electrolytes (S2 and S4, Li^+: 1.5 mol kg^{-1}). As shown in Fig. 6, the ionic conduction mechanism of the gel polymer electrolytes should
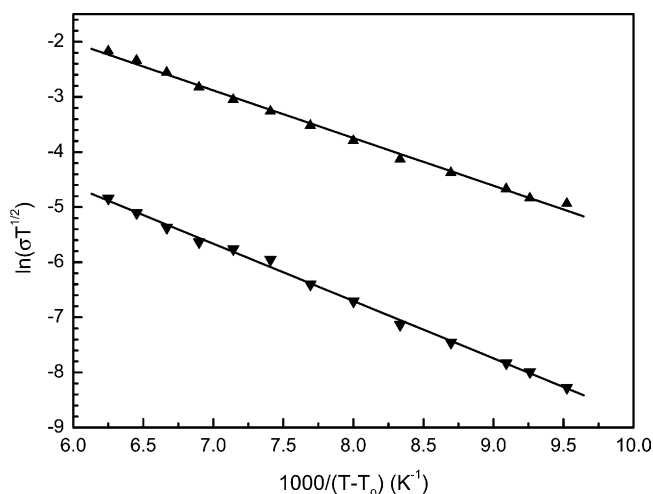
Fig. 6. VTF plots of ionic conductivity for composite polymer electrolytes added with LiClO$_4$: (▼) S2 and (▲) S4, in which Li$^+$ content is 1.5 mol kg^{-1}.

follow Vogel–Tamman–Fulcher (VTF) equation [28]:

$$\sigma = AT^{-1/2} \exp\left(-\frac{E_0}{k(T - T_0)}\right) \qquad (4)$$

where A is a pre-exponential factor which may be related to ion mobility and ion association, E_0 an apparent activation energy, which is different from the activation energy, E, obtained by the Arrhenius equation, k a Boltzmann's constant, and T_0 is an apparent transition temperature, T_g, of the electrolyte and has been reported to be 35–50 °C lower than T_g for many polymer electrolyte systems.

Since the VTF dependence is characteristic for the composite polymer electrolytes, it seems that the flexibility of polymer chains, characteristic for amorphous regions of comb-like copolymer, partially determines the ionic conductivity. Results of a more detailed study of the ionic conductivity and phase behavior of electrolytes based on the copolymers will soon be reported.

4. Conclusion

In this work, we present a novel comb-like copolymer PEGMEMA–AN–MMA and LiClO$_4$ composite polymer electrolyte system. The copolymer is capable of forming donor:acceptor type bonds with Li$^+$. The complex is associated with a mixture of SiO$_2$ or PC. These polymer electrolytes were studied using DSC, FT-IR, NMR, AFM, and EIS. Such electrolytes possess satisfactory ambient temperature ionic conductivity (up to 10^{-4} S cm^{-1}) and good mechanical strength, which satisfy the practical requirements for lithium batteries. The EIS studies illustrate that the ionic conductivity of these hybrid polymer electrolytes was found to depend on the Li$^+$ content, the addition of fumed silica, and the plasticizer PC. The results could be attributed to the addition of SiO$_2$, which has an obvious effect on morphology

and thermal properties of polymer electrolyte. The nature of fumed SiO$_2$ did not influence the ionic conductivity of pure polymer electrolyte significantly. The ionic conductivity of polymer electrolyte increases largely after impregnated with PC, especially for the polymer electrolytes with SiO$_2$. The polymer electrolyte investigated in this work shows VTF behavior, indicating that the Li$^+$ ion motion is depended on the flexibility of the polymer chain.

References

[1] J.M. Tarascon, M. Armand, Nature 414 (2001) 359.
[2] P. Lightfoot, M.A. Metha, P.G. Bruce, Science 262 (1993) 883.
[3] K.M. Abraham, Electrochim. Acta 38 (1993) 1233.
[4] P.G. Bruce, Electrochim. Acta 40 (1995) 2077.
[5] Z. Gadjourova, Y.G. Andreev, D.P. Tunstall, P.G. Bruce, Nature 412 (2001) 520.
[6] Z. Bashir, S.P. Church, D.M. Price, Acta Polym. 44 (1993) 211.
[7] Y.K. Yarovoy, H.P. Wang, S.L. Wunder, Solid State Ionics 118 (1999) 301.
[8] H.P. Wang, H. Huang, S.L. Wunder, J. Electrochem. Soc. 147 (2000) 2853.
[9] K. Murata, S. Izuchi, Y. Yoshihisa, Electrochim. Acta 45 (2000) 1501.
[10] P.M. Blonsky, D.F. Shriver, P.E. Austin, H.R. Allcock, J. Am. Chem. Soc. 106 (1984) 6854.
[11] J.R.M. Giles, F.M. Gray, J.R. MacCallum, C.A. Vincent, Polymer 28 (1987) 1977.
[12] H.M. Nekoomanesh, S. Nagae, C. Booth, J.R. Owen, J. Electrochem. Soc. 139 (1992) 3046.
[13] C.W. Walker Jr., M. Salomon, J. Electrochem. Soc. 140 (1993) 3409.
[14] D.J. Bannister, G.R. Davies, I.M. Ward, J.E. McIntyre, Polymer 25 (1984) 1600.
[15] A. Nishimoto, K. Agehara, N. Furuya, T. Watanabe, M. Watanabe, Macromolecules 32 (1999) 1541.
[16] M. Kono, M. Nishiura, E. Ishiko, T. Sada, Electrochim. Acta 8/9 (2000) 1307.
[17] U. Lauter, W.H. Meyer, G. Wegner, Macromolecule 30 (1997) 2092.
[18] J.Y. Song, Y.Y. Wang, C.C. Wan, J. Power Sources 77 (1999) 183.
[19] X. Liu, T. Osaka, J. Electrochem. Soc. 144 (1997) 3066.
[20] S. Rajendran, T. Mahalingam, R. Kannan, Solid State Ionics 130 (2000) 143.
[21] L. Qi, Y.Q. Lin, F.S. Wang, Solid State Ionics 109 (1998) 145.
[22] L. Qi, Y.Q. Lin, X.B. Jing, F.S. Wang, Solid State Ionics 139 (2001) 293.
[23] W.H. Hou, C.Y. Chen, C.C. Wang, Polymer 44 (2003) 2983.
[24] J.R. Macdonald, J. Chem. Phys. 61 (1974) 3977.
[25] R.O. Ansel, T. Dickinson, A.F. Povy, P.M.A. Sherwood, J. Elelctrohcem. Soc. 124 (1977) 1360.
[26] M.J. Rodiguez Presa, R.I. Tuueri, M.I. Florit, D. Posaldas, J. Electroanal. Chem. 82 (2001) 502.
[27] S. Petrucci, E.M. Eyring, J. Phys. Chem. 95 (1991) 1731.
[28] Ib.L. Olsen, R. Koksbang, J. Electrochem. Soc. 143 (1996) 570.